

# A Dual Responsive Probe Based on Bromo Substituted Salicylhydrazone Moiety For The Colorimetric Detection of Cd<sup>2+</sup> Ions and Fluorometric Detection of F<sup>-</sup> Ions: Applications In Live Cell Imaging

Krishnaveni Karupiah, Iniya Murugan, Murugesan Sepperumal, and Siva Ayyanar<sup>a\*</sup>

<sup>a</sup>Supramolecular and Organometallic Chemistry Laboratory, Department of Inorganic Chemistry, School of Chemistry, Madurai Kamaraj University, Madurai-625021, Tamil Nadu, India.

## ARTICLE INFO

### Article history:

Received 20210217

Received in revised form 20210310

Accepted 20210317

Available online 20210405

### Keywords:

5-Bromosalicyl hydrazine;

Colorimetric;

DFT;

Hela cells;

Zebrafish embryos

## ABSTRACT

A new fluorimetric and colorimetric dual-mode probe, 4-bromo-2-(hydrazonomethyl) phenol (**BHP**) has been synthesized and successfully utilized for the recognition of Cd<sup>2+</sup>/F<sup>-</sup> ions in DMSO/H<sub>2</sub>O (9:1, v/v) system. The probe displays dual channel of detection via fluorescence enhancement and colorimetric changes upon binding with F<sup>-</sup> and Cd<sup>2+</sup> ions respectively. The Job's plot analysis, ESI-MS studies, Density Functional Theoretical (DFT) calculations, <sup>1</sup>H NMR and <sup>19</sup>F NMR titration results were confirmed and highly supported the 1:1 binding stoichiometry of the probe was complexed with Cd<sup>2+</sup>/F<sup>-</sup> ions. Furthermore, intracellular detection of F<sup>-</sup> ions in HeLa cells and fluorescence imaging analysis in Zebrafish embryos results of the probe **BHP** might be used to reveal their potential applications in a biological living system.

**2021 SciForce Publications. All rights reserved.**

\*Corresponding author: E-mail: [drasiva@gmail.com](mailto:drasiva@gmail.com), [siva.chem@mkuniversity.org](mailto:siva.chem@mkuniversity.org) (A. Siva)

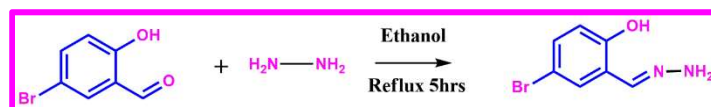
Tel. +91-452-2458471/346, Fax. +91-452-2459181

## Introduction

The quantification and detection of toxic metal ions in diverse fields have fascinated more attention in recent years due to their prominent and significant roles in clinical diagnosis and ecological system.<sup>1-6</sup> Besides metal ions, anions also play an exclusive role in a variety of chemical and biological processes.<sup>7-12</sup> In earlier, analytical methods for the detection of cations/anions has required highly sophisticated and expensive instruments such as atomic absorption spectrometry, inductively coupled plasma mass spectrometry, ion sensitive electrodes, and gas and ion chromatography. Amid, fluorescent techniques have more expedient in terms of rapidness, excellent sensitivity and selectivity, low cost, easy and feasible detection. In addition, optical detection mode analysis is a more appropriate method because of their potential features such as easy handling, real-time analysis and different signal output modes.<sup>13-16</sup> Besides, colorimetric assays are more feasible and potent tool as they provide a simple visible authentication for analyte detection in the absence of instruments and tedious techniques. In this perspective, the recent research area has been mainly focused to design the novel multi-functional fluorometric and colorimetric sensors for the detection of ions in the different environments.

Cadmium (Cd<sup>2+</sup>) is one of the important hazardous heavy transition metal ions<sup>17</sup> in the environment due its carcinogenic nature. The higher accumulation of Cd<sup>2+</sup> ion and inhalation of

Cd-dust prompts more awful health issues in human like cancer, cardiovascular diseases, kidneys and liver damage.<sup>18</sup> Furthermore, the Cd<sup>2+</sup> ion has more advantages in several industries such as pigments in plastics, electroplating and batteries, etc. On the other hand, fluoride ions play an ample role in dental health and in the treatment of osteoporosis.<sup>19-22</sup> The excess of fluoride ingestion prompted severe disease in human health like gastric and kidney problems.<sup>23</sup> In some remote areas, the high level contamination of fluoride ions in drinking water triggered bone disease such as fluorosis.<sup>24-31</sup> Thus, to develop and synthesize novel multifunctional probe for the detection and quantification of both cations and anions is a highly anticipated and imperative task.



**Scheme 1. Synthesis of probe BHP**

Herein, we have fabricated and synthesized a novel chromogenic and fluorogenic assay based on bromo substituted salicylhydrazone moiety for the colorimetric and fluorometric detection of F<sup>-</sup> ions and colorimetric detection of Cd<sup>2+</sup> ions in DMSO/H<sub>2</sub>O (9:1, v/v) system. The UV-visible and fluorescence spectral analysis of **BHP** with Cd<sup>2+</sup>/F<sup>-</sup> ions exposed an

outstanding ratiometric absorbance and colorimetric responses towards F<sup>-</sup> ions and also showed a visible colorimetric response towards Cd<sup>2+</sup> ions. The fluorescence enhancement of **BHP** with F<sup>-</sup> ion was highly evaluated by DFT calculations. As well, the cell viability experimental results of **BHP** can be used for the detection of F<sup>-</sup> ions in both HeLa cells and Zebrafish embryos via high content analysis system.

## Experimental Methods

### Materials

All the chemicals used in the present study were in the analytical reagent grade and solvents used were of HPLC grade. Reagents were used as such received without any further purification. Metal ions such as K<sup>+</sup>, Na<sup>+</sup>, Ca<sup>2+</sup>, Mg<sup>2+</sup>, Fe<sup>2+</sup>, Fe<sup>3+</sup>, Ag<sup>+</sup>, Zn<sup>2+</sup>, Mn<sup>2+</sup>, Cu<sup>2+</sup>, Co<sup>2+</sup>, Ni<sup>2+</sup>, Cd<sup>2+</sup>, Al<sup>3+</sup>, Cr<sup>3+</sup>, Pb<sup>2+</sup> and Hg<sup>2+</sup> were purchased from Merck and S.D. Fine chemicals. The anions of Cl<sup>-</sup>, Br<sup>-</sup>, I<sup>-</sup>, SCN<sup>-</sup>, CN<sup>-</sup>, H<sub>2</sub>PO<sub>4</sub><sup>-</sup>, HSO<sub>4</sub><sup>-</sup>, NO<sub>3</sub><sup>-</sup>, AcO<sup>-</sup> and F<sup>-</sup> were purchased as their tetrabutylammonium salts from Sigma-Aldrich Pvt. Ltd. Absorption measurements were performed on JASCO V-630 spectrophotometer in 1 cm path length quartz cuvette with a volume of 2 mL at room temperature. Fluorescence measurements were made on a JASCO and F-4500 Hitachi Spectrofluorimeter with excitation slit set at 5.0 nm band pass and emission at 5.0 nm band pass in 1 cm × 1 cm quartz cell. <sup>1</sup>H and <sup>13</sup>C NMR spectra were obtained on a Bruker 300 MHz NMR instrument with TMS as internal reference using DMSO-*d*<sub>6</sub> as solvent. Standard Bruker software was used throughout. <sup>19</sup>F NMR spectra were recorded at 293K on BRUKER 400 MHz FT-NMR spectrometers using DMSO-*d*<sub>6</sub> as solvent. ElectroSpray Ionisation Mass Spectrometry (ESI-MS) analysis was performed in the positive/negative ion mode on a liquid chromatography-ion trap mass spectrometer (LCQ Fleet, Thermo Fisher Instruments Limited, US). Fluorescence microscopic imaging measurements were determined using Operetta High Content Imaging System (PerkinElmer, US)

### Synthesis of (*E*)-4-bromo-2-(hydrazonomethyl) phenol, **BHP**

An absolute alcoholic solution (50 ml) of 5-bromosalicylaldehyde (0.5 gm, 2.49 mmol) was refluxed under hydrazine hydrate (in excess) for 5 hr and the pale yellow color solid product was collected after recrystallized with ethanol and ethyl acetate mixture (yield, 95 %). <sup>1</sup>H NMR (300 MHz, DMSO-*d*<sub>6</sub>) δ (ppm): 8.92 (s, 1H), 11.89 (s, 1H), 7.53 (d, *J* = 8.7 Hz, 1H), 6.94 (d, *J* = 5.8 Hz, 1H); <sup>13</sup>C NMR (75 MHz, DMSO-*d*<sub>6</sub>) δ (ppm): 161.36, 158.51, 135.84, 131.82, 120.86, 119.69, 106.72.

### Photophysical analysis of **BHP**

The optical mode analysis of **BHP** towards various cations/anions in DMSO/H<sub>2</sub>O (9:1, v/v) system was carried out by using absorbance and fluorescence spectroscopy. UV-visible and fluorescence analysis of **BHP** with cations were gauged by using their corresponding acetate salts of metal ions. Tetrabutylammonium salts of competing anions were used for the anionic sensing analysis.

### Computational Studies

The optimized geometrical and ground state energy level calculations of **BHP** were obtained by Density functional theoretical (DFT) calculations were executed using Gaussian 09 program<sup>32</sup> with the 6-311G basis set. The optimized geometries and the fluorescence enhancement of probe **BHP** complexed with Cd<sup>2+</sup>/F<sup>-</sup> ions were attained by DFT-B3LYP level theory using 6-311G and LANL2DZ basis sets.

### Cytotoxicity studies

HeLa cell lines were procured from the National Center for Cell Science (NCCS), Pune, India. Cell lines are kept in the Dulbecco's Modified Eagle's medium (DMEM) supplemented with 10% fetal bovine serum (FBS), 1% antimycotic and antibiotic solution was used in this study. The cells were kept in an incubator at 25 °C with humidified atmosphere comprising 5% of CO<sub>2</sub> and 95% of air. HeLa cells were loaded over the wells of 96 well-culture plates with a density of 1 × 10<sup>4</sup> cells/well. After 48 h of incubation, previous DMEM medium was exchanged with new medium and **BHP** (dissolved in DMSO) was added in the range of 0-200 μM to all the wells and further incubated over 3h. Cytotoxicity of **BHP** was measured by using MTT [3-(4,5-dimethylthiazol-2-yl)-2,5-diphenyltetrazolium bromide] assay. After incubation of HeLa cells with **BHP**, the medium was detached. Further, 100 μl of DMSO was added and the resulting formazan crystals were dissolved in DMSO. The cell viability was determined by measuring the absorbance of each well at 540-660 nm (formation of formazan) using a microplate reader.

### In vivo fluorescence analysis in Zebrafish embryos

The fluorescence imaging analysis was performed in four days old embryos. The embryos were seeded over F<sup>-</sup> ion alone for 2 h in the E3 medium. The E3 medium was prepared by dissolving 5.0 mM NaCl, 0.17 mM KCl, 0.33 mM CaCl<sub>2</sub>, 0.33 mM MgSO<sub>4</sub> ingredients in H<sub>2</sub>O (2L) and the pH 7.2 was adjusted by adding NaOH. The embryos were thoroughly washed with E3 medium. Successively, incubated embryos were sowed over 25 μM of **BHP** (in DMSO) solution for 3h. Further, embryos were washed again with E3 medium and fixed in 10% methyl cellulose solution for the good oriented images. The fluorescent images of **BHP**-F<sup>-</sup> were logged using high content screening microscopy. (Excitation wavelength of 482 nm and emission wavelength range of 500-700 nm).

### Results and discussion

The probe, (*E*)-4-bromo-2-(hydrazonomethyl) phenol (**BHP**) has been synthesized by one step condensation between hydrazine and 5-bromosalicylaldehyde in ethanol (yield, 95 %) as shown in Scheme 1. The structure of the probe **BHP** was confirmed via <sup>1</sup>H, <sup>13</sup>C NMR analysis (Figure S1-S2, See ESI)

### UV-vis spectral analysis of cations with **BHP**

To investigate the cation sensing events of **BHP** towards different cations in DMSO/H<sub>2</sub>O (9:1, v/v) system by using UV-

vis and fluorescence titration experiments. Initially, free probe **BHP** exhibited an absorption band at 367 nm and further addition of mono, di and trivalent cations such as  $\text{Li}^+$ ,  $\text{K}^+$ ,  $\text{Ag}^+$ ,  $\text{Mn}^{2+}$ ,  $\text{Co}^{2+}$ ,  $\text{Ni}^{2+}$ ,  $\text{Cu}^{2+}$ ,  $\text{Zn}^{2+}$ ,  $\text{Fe}^{2+}$ ,  $\text{Hg}^{2+}$ ,  $\text{Na}^+$ ,  $\text{Mg}^{2+}$ ,  $\text{Ca}^{2+}$ ,  $\text{Pb}^{2+}$ ,  $\text{Fe}^{3+}$  and  $\text{Cr}^{3+}$  exhibited tiny changes in absorption spectrum due to their weak interaction towards **BHP** except  $\text{Cd}^{2+}$  ion as shown in Figure 1. Interestingly, upon titrated with  $\text{Cd}^{2+}$  ion, a new absorption band appeared at 470 nm due to the highly resonance induced charge transfer ability of bromo substituted salicyl moiety while the solution turns into dark yellow color from pale yellow. Increasing addition of  $\text{Cd}^{2+}$  ion results gradual reduction of both higher and lower energy bands at 367 nm and 470 nm respectively as depicted in Figure 2.

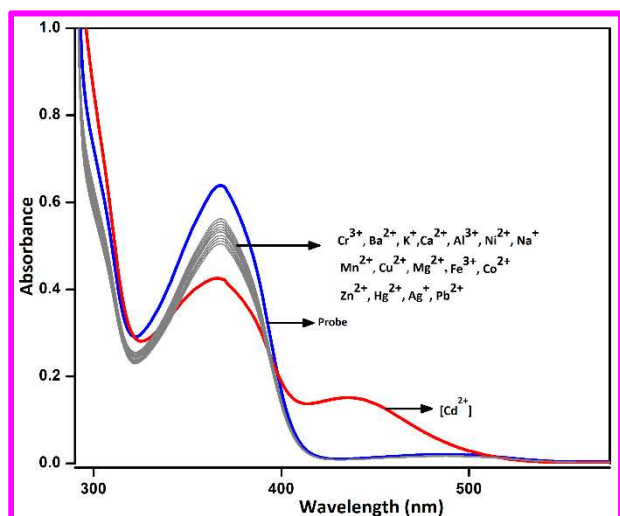


Figure 1. UV-vis spectra of BHP (10  $\mu\text{M}$ ) with different cations ( $5 \times 10^{-3}$  M) in DMSO/ $\text{H}_2\text{O}$  (9: 1, v/v) system.

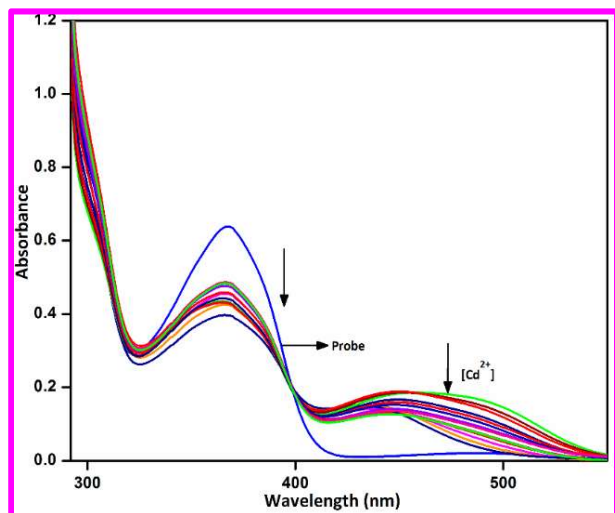


Figure 2. UV-vis spectra of BHP (10  $\mu\text{M}$ ) with  $\text{Cd}^{2+}$  (0 – 100  $\mu\text{M}$ ) in DMSO/ $\text{H}_2\text{O}$  (9: 1, v/v) system

Besides, fluorescence response of probe **BHP** towards various cations such as  $\text{Li}^+$ ,  $\text{K}^+$ ,  $\text{Ag}^+$ ,  $\text{Mn}^{2+}$ ,  $\text{Co}^{2+}$ ,  $\text{Ni}^{2+}$ ,  $\text{Cu}^{2+}$ ,  $\text{Zn}^{2+}$ ,  $\text{Fe}^{2+}$ ,  $\text{Hg}^{2+}$ ,  $\text{Na}^+$ ,  $\text{Mg}^{2+}$ ,  $\text{Ca}^{2+}$ ,  $\text{Pb}^{2+}$ ,  $\text{Fe}^{3+}$  and  $\text{Cr}^{3+}$  including  $\text{Cd}^{2+}$  ion have been inspected in DMSO/ $\text{H}_2\text{O}$  (9:1, v/v) system. Initially, the probe **BHP** displayed low intense fluorescence band in free state. Addition of other commonly coexistent metal ions including  $\text{Cd}^{2+}$  ions exhibited trivial changes in fluorescence spectra. From these results, it is concluded that the probe **BHP** could serve as an excellent colorimetric assay for the detection of  $\text{Cd}^{2+}$  ions.

### The sensing analysis of BHP towards anions

Moreover, the anion binding attraction of **BHP** towards anions have been investigated in DMSO/ $\text{H}_2\text{O}$  (9:1, v/v) system via both UV-visible and fluorescence spectral techniques. Initially the probe **BHP** showed the absorption band at 367 nm. Upon titrated with other anions such as  $\text{Cl}^-$ ,  $\text{Br}^-$ ,  $\text{I}^-$ ,  $\text{NO}_3^-$ ,  $\text{AcO}^-$ ,  $\text{HSO}_4^-$ ,  $\text{H}_2\text{PO}_4^-$  and  $\text{CN}^-$  were failed to alter the absorbance of the probe **BHP** except  $\text{F}^-$  ions as shown in Figure 3a. Moreover, the incremental addition of  $\text{F}^-$  ions (0-50  $\mu\text{M}$ ), the higher energy band at 367 nm was decreased along with the increment in new absorption band at 482 nm results an excellent ratiometric response. The new low energy band observed at 482 nm due to the deprotonation of  $-\text{OH}$  group present in salicyl moiety initiated by hydrogen bonding [Figure 3b]. At that affair, the solution turns into orange color from pale yellow and it was simply discerned by naked eye [Figure 4].

Besides, under identical condition, the fluorescence titration experiment of **BHP** was carried out in the presence of different anions. Interestingly, the probe **BHP** displayed low intense fluorescence band at 601 nm and the other competing anions were failed to affect the fluorescence intensity except  $\text{F}^-$  ions as shown in [Figure 5a]. Further, the incremental addition of  $\text{F}^-$  ions triggers the enhancement in intensity results an excellent “turn on” fluorescence response due to the deprotonation and the inhibition of charge transfer state stimulated by resonance around the moiety [Figure 5b].

### Competitive experiments

To gauge the selectivity and recognizing ability of **BHP**, competitive analysis was performed in the presence of varying concentration of  $\text{F}^-$  ion (0-50  $\mu\text{M}$ ). Initially, the probe was treated with  $5 \times 10^{-3}$  M of different anions such as  $\text{CN}^-$ ,  $\text{I}^-$ ,  $\text{Br}^-$ ,  $\text{Cl}^-$ ,  $\text{NO}_2^-$ ,  $\text{CH}_3\text{COO}^-$ ,  $\text{H}_2\text{PO}_4^-$  and  $\text{HSO}_4^-$ . The other common competing anions were failed to bind with the probe **BHP** except  $\text{F}^-$  ion [Figure 6 (a) and (b)]. From these observations, it is ensured that **BHP** could act as an excellent selective and sensitive chromogenic receptor for  $\text{F}^-$  ions in real time monitoring and different biological applications.

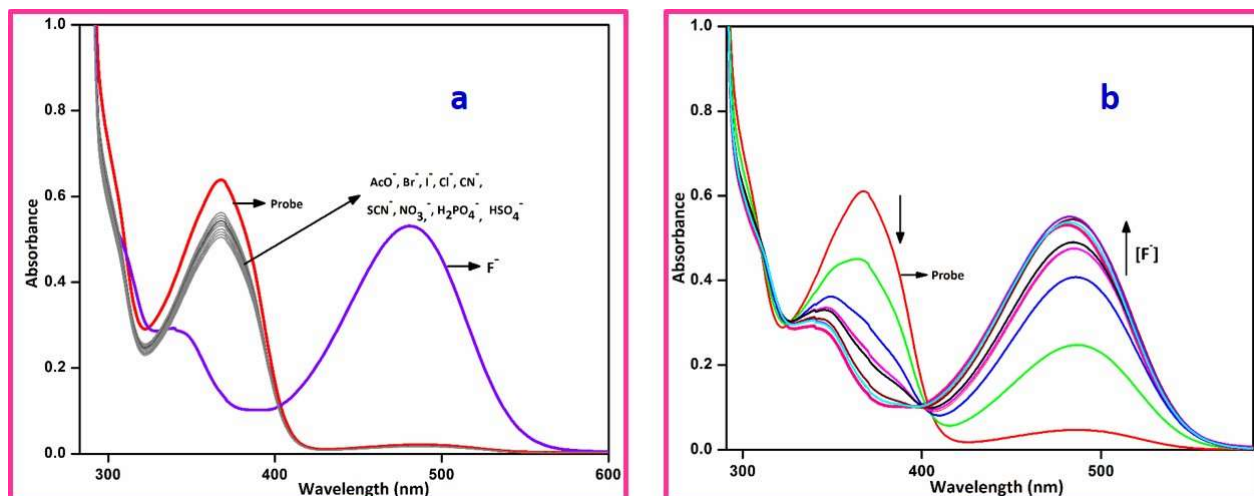


**Figure 3 (a):** UV-vis spectra of BHP with  $5 \times 10^{-3}$  M of other anions in DMSO/H<sub>2</sub>O (9: 1 v/v) system. (b) UV-visible spectra of BHP (5  $\mu$ M) with F<sup>-</sup> (0-50  $\mu$ M) in DMSO/H<sub>2</sub>O (9: 1 v/v) system.

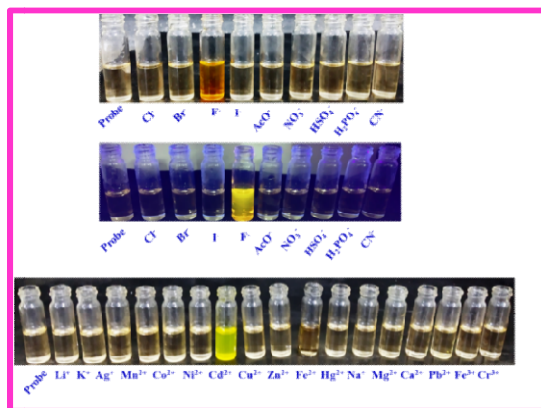


**Figure 4.** Naked eye detection of F<sup>-</sup> ions with BHP under visible light (top) and UV-lamp (bottom) and BHP with Cd<sup>2+</sup> visible light only (bottom).

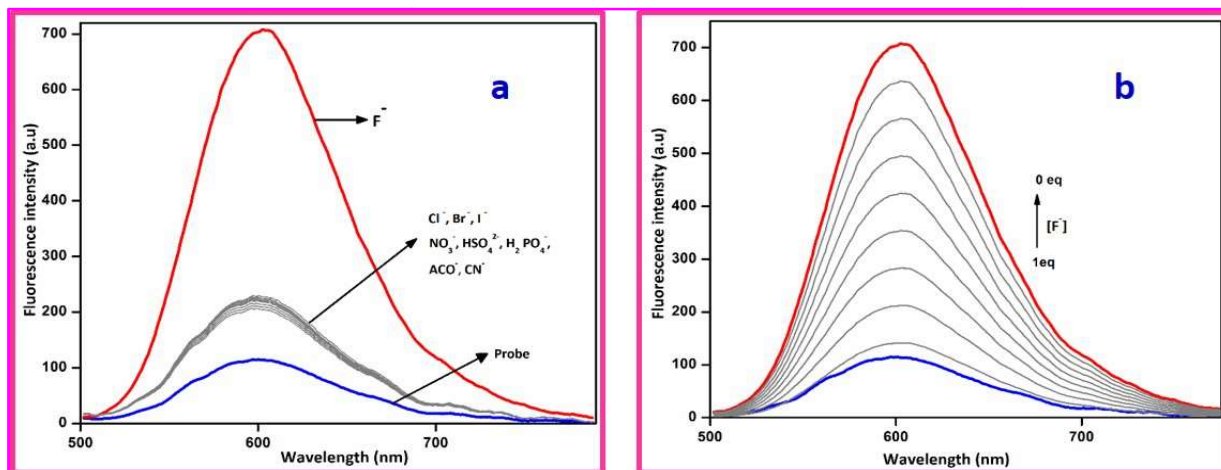


**Figure 5 (a):**Fluorescence spectra of BHP (5 $\mu$ M) with  $5 \times 10^{-3}$  M of other anions in DMSO/H<sub>2</sub>O (9: 1, v/v) system. Excitation at 482 nm. Slit width is 5 nm. (b) Fluorescence spectra of BHP (5 $\mu$ M) with F<sup>-</sup> (0-50  $\mu$ M) in DMSO/H<sub>2</sub>O (9: 1, v/v) system. Excitation at 482 nm. Slit width is 5 nm.

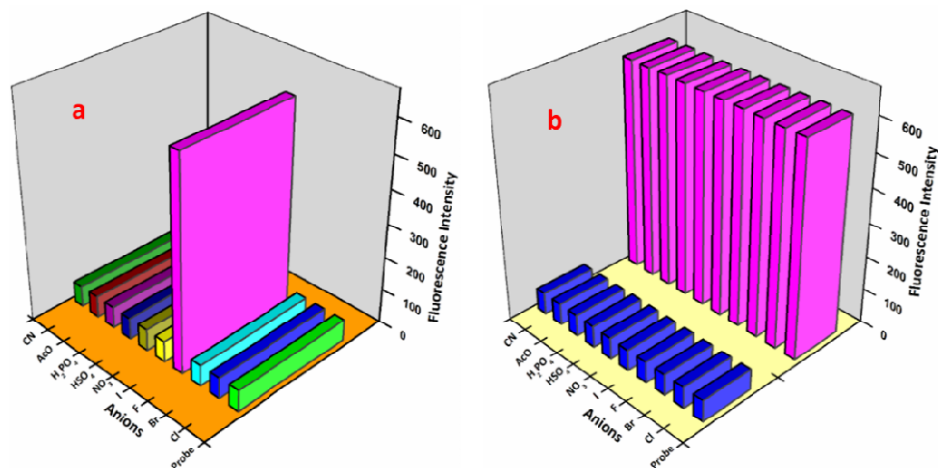


**Figure 6 (a):**Selectivity analysis of F<sup>-</sup> ion with BHP in the presence of competing anions. Excitation at 480 nm, Slit width = 5 nm. (b) The blue bars represent the change of the fluorescence intensity of BHP with the consequent addition of other anions. The pink bars represent the addition of the competing anions to BHP. Excitation at 480 nm, Slit width = 5 nm.

### Job's plot analysis and calculation of binding constant of BHP for Cd<sup>2+</sup>/F<sup>-</sup> ions

Furthermore, the Job's plot [Figure 7(a) and (b)] analysis based on UV-visible and fluorescence titration experiments results confirmed the 1:1 binding stoichiometry of **BHP** with both Cd<sup>2+</sup>/F<sup>-</sup> ions respectively. To further support the binding stoichiometry of **BHP** with Cd<sup>2+</sup>/F<sup>-</sup> ions, ESI-MS spectral analysis were performed. The ESI-MS spectral analysis of **BHP**-Cd<sup>2+</sup>/**BHP**-F<sup>-</sup> disclosed peaks at 327.45/258.28 corresponds to [BHP+Cd<sup>2+</sup>+Na<sup>+</sup>]/[BHP+F<sup>-</sup>+H<sup>+</sup>+Na<sup>+</sup>] respectively (Figure S3-S4, See ESI). Furthermore, the 1:1 binding stoichiometry of **BHP** with F<sup>-</sup> ions was confirmed via <sup>1</sup>H NMR titration profile (Figure 8) and <sup>19</sup>F NMR. The deprotonation of -OH group present in the salicyl moiety was initiated by hydrogen bonding and the plausible binding mode of **BHP** with Cd<sup>2+</sup> and F<sup>-</sup> ion is shown in Scheme 2. Further, the absorbance and fluorescence

intensity changes of Cd<sup>2+</sup> ions (A<sub>472 nm</sub>) and F<sup>-</sup> ions (A<sub>482 nm</sub>, I<sub>603 nm</sub>) were plotted against [Cd<sup>2+</sup>] and [F<sup>-</sup>] respectively provided a good linear relationship between both **BHP** and Cd<sup>2+</sup>/F<sup>-</sup> ions (Figure S5, S6 and S7, See ESI).

From absorbance and fluorescence titration profile, the binding constant values of **BHP** for Cd<sup>2+</sup>/F<sup>-</sup> ions were calculated using modified Benesi-Hildebrand method ions (Figure S8, S9 and S10, See ESI). The binding constant values of **BHP** with Cd<sup>2+</sup> ions were found to be 4.26 × 10<sup>4</sup> M from UV-visible titration profile. Similarly, the binding constant values of **BHP** with F<sup>-</sup> ions were estimated to be 6.03 × 10<sup>-3</sup> M / and 3.01 × 10<sup>-4</sup> M from UV-visible and fluorescence titration profile respectively. The detection limits (LOD) of F<sup>-</sup> were calculated to be 0.05 nM respectively. Moreover, the LOD values of **BHP** signifies that the probe might be utilized for the quantitative determination of F<sup>-</sup> ions in environment and real system.

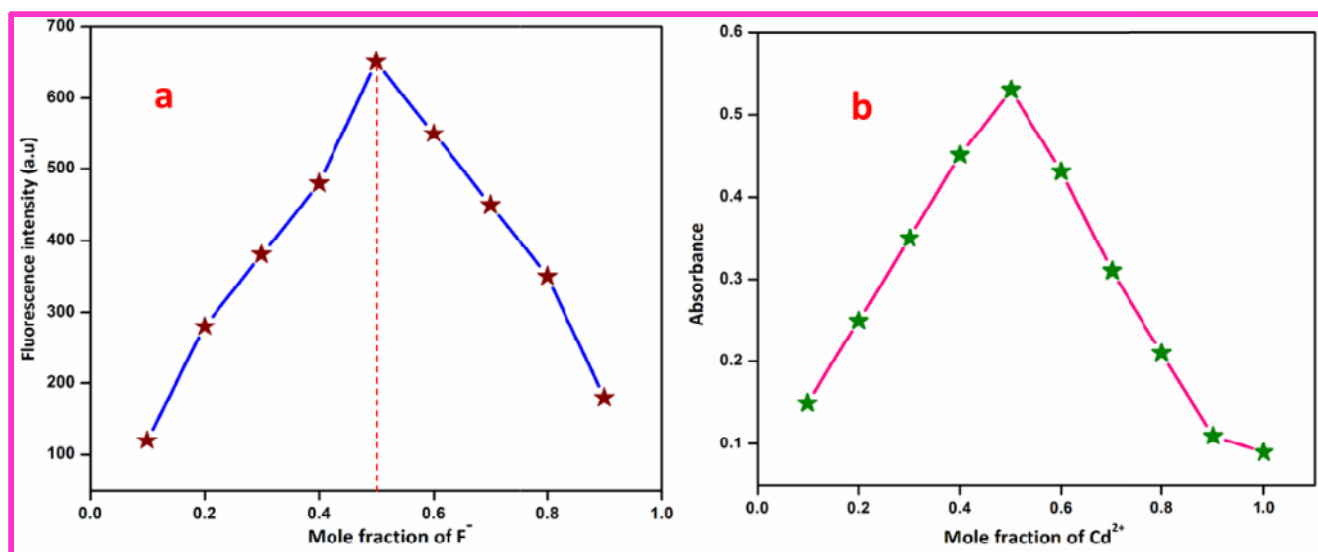
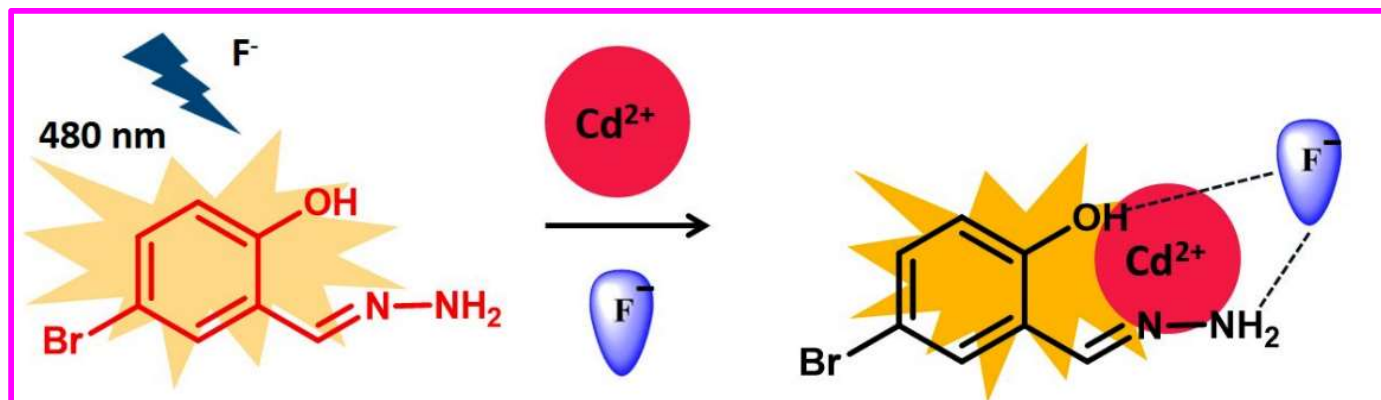


**Figure 7 (a)** Job's plot for BHP with F<sup>-</sup> ion. (b) Job's plot for BHP with Cd<sup>2+</sup> ion



Scheme 2. Binding mode of BHP with Cd<sup>2+</sup>/F<sup>-</sup> ions

### <sup>1</sup>H NMR titrations of BHP with F<sup>-</sup> ions

In addition, to confirm and highly supported the 1:1 binding stoichiometry of probe with F<sup>-</sup> ions, <sup>1</sup>H NMR titrations was performed. Upon addition of F<sup>-</sup> ion (0.5 equiv), the proton signal corresponds to phenolic -OH group at 11.14 ppm was gradually

decreased. Further, addition of 1 equiv. of F<sup>-</sup> ions to **BHP** showed the complete disappearance of -OH proton signal as depicted in Figure 8. Moreover, the binding stoichiometric ratio of F<sup>-</sup> ion with **BHP** was further supported by <sup>19</sup>F NMR experiment. The (H<sub>2</sub>F)<sup>-</sup> signal appeared at -124.33 ppm (Figure S11-S12, See ESI) confirms the deprotonation process arose from phenolic -OH proton.

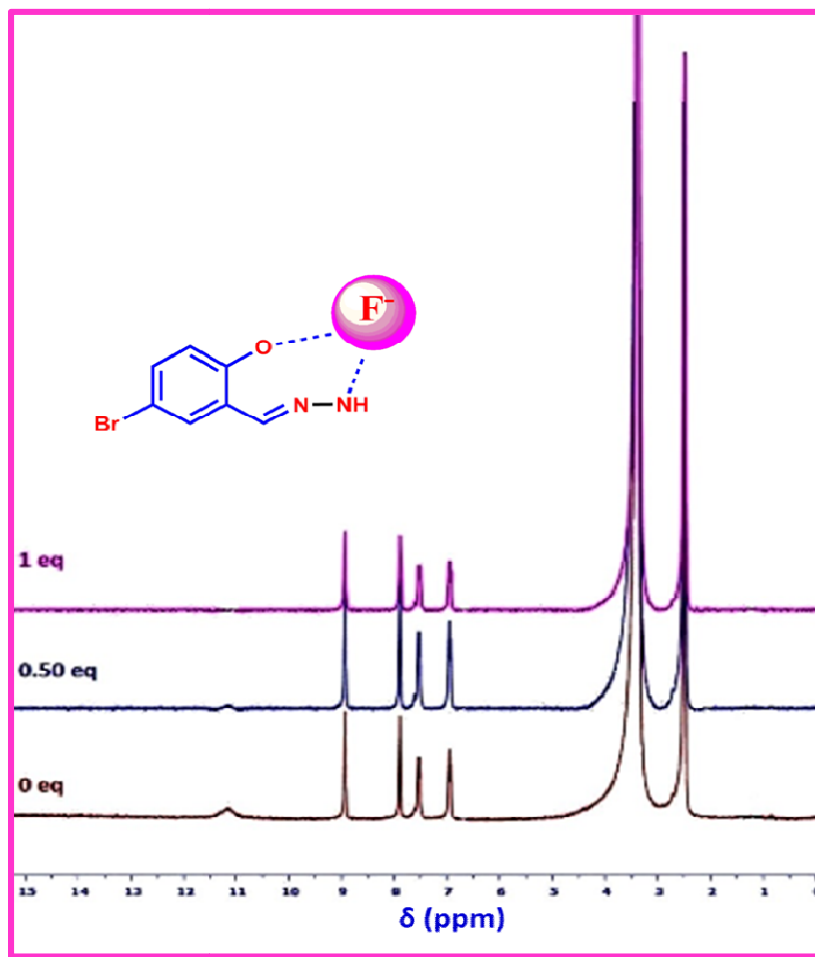


Figure 8 <sup>1</sup>H NMR titration of BHP with F<sup>-</sup> (0-1equiv) in DMSO-*d*<sub>6</sub>

### DFT calculations of BHP with $\text{Cd}^{2+}/\text{F}^-$ ion

To recognize the fluorescence enhancement of probe **BHP** after complexation with  $\text{F}^-$ , DFT calculations were accomplished. The optimized structures of **BHP**, **BHP- $\text{Cd}^{2+}$**  and **BHP- $\text{F}^-$**  were obtained using DFT/B3LYP-6-311G and B3LYP/LanL2DZ basis sets respectively. The frontier molecular orbital diagram obtained from optimized structure of **BHP** is presented in Figure 9. Upon binding with  $\text{Cd}^{2+}$  ion, the HOMO

and LUMO are delocalized over the entire salicyl unit and their energy gap was reduced. It is noteworthy that inhibition of charge transfer in probe **BHP** renders the reduction of absorbance at 367 nm and 470 nm. Moreover, Complexation of  $\text{F}^-$  ion to the probe **BHP** leads to lowering of HOMO-LUMO energy gap. In the presence of  $\text{F}^-$ , HOMO and LUMO are distributed over the whole molecule of **BHP**. From these results, the  $\text{F}^-$  ion was efficiently binded and complexed with **BHP** than  $\text{Cd}^{2+}$  ion.

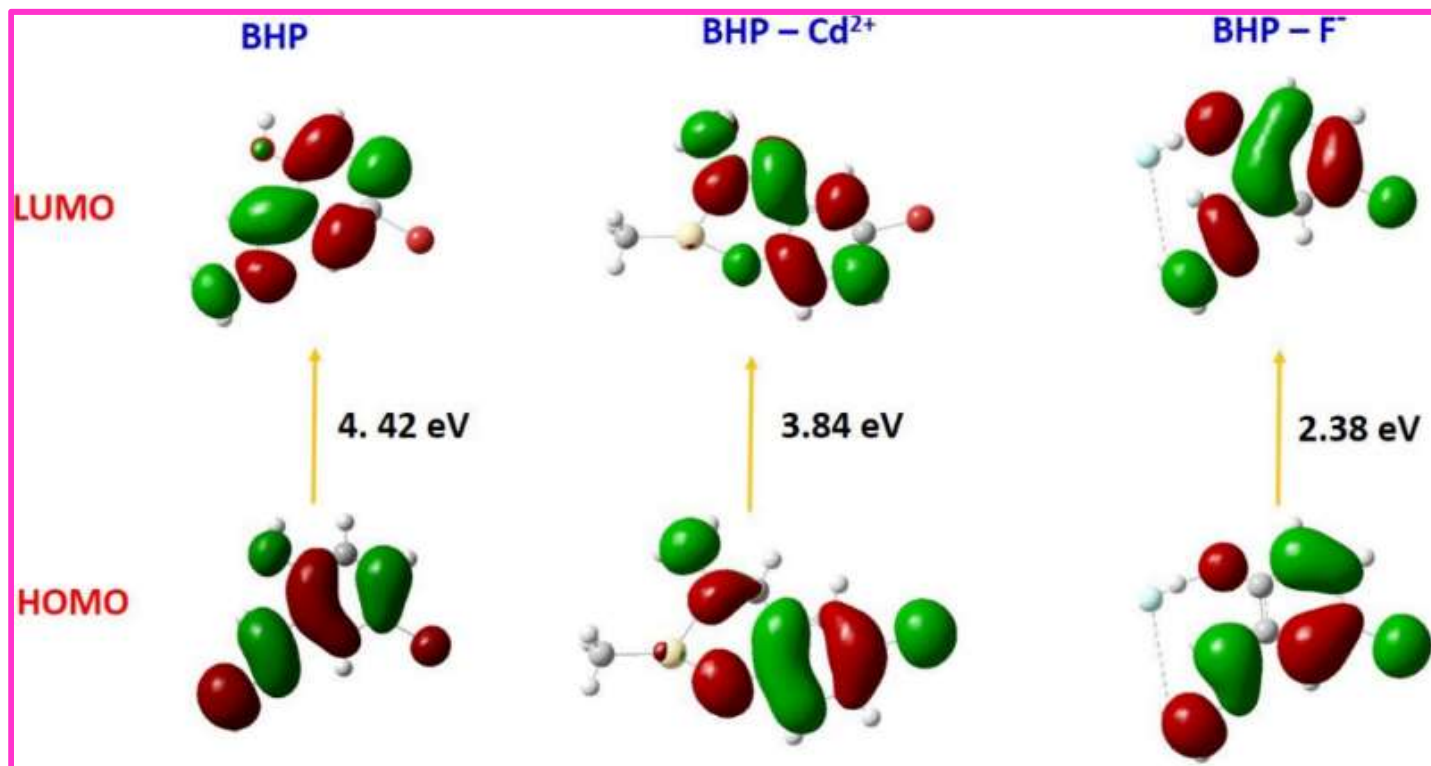
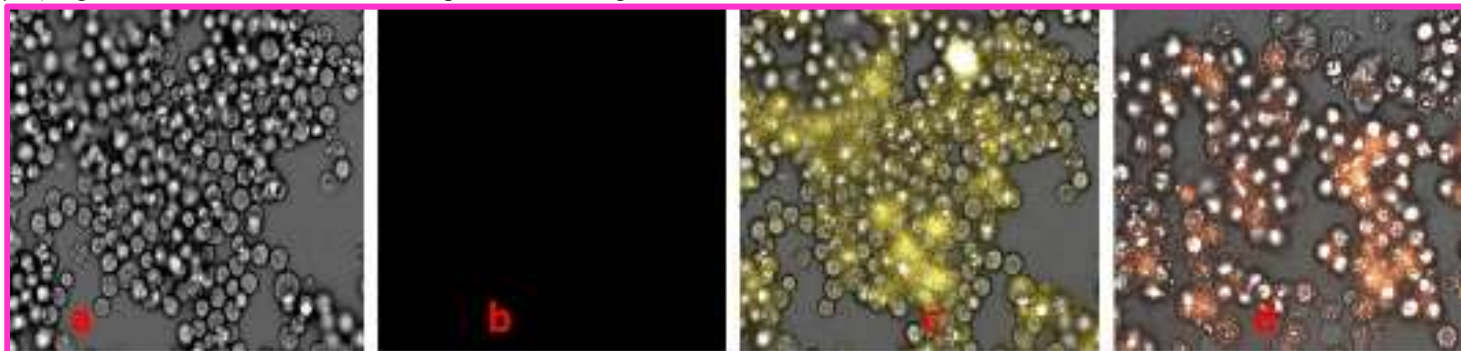


Figure 9. Frontier molecular orbital diagram of BHP, BHP- $\text{Cd}^{2+}$  and BHP- $\text{F}^-$

### Live cell Imaging analysis of BHP in HeLa cells / Zebrafish embryos

The cell viability or cytotoxicity analysis of **BHP** (0–200  $\mu\text{M}$ ) against Human HeLa cells were performed using MTT

assay. In 100  $\mu\text{M}$  of **BHP**, cell viability was obtained as too high as 98%. (Figure S13, See ESI). Hence, the probe was successfully used for live cell imaging analysis of  $\text{F}^-$  ions in



**Figure 10.** Live cell fluorescence imaging analysis of BHP in HeLa cells. (a) Bright field images of HeLa cells incubated with BHP (25  $\mu\text{M}$ ) for 3h (b) Fluorescence merged images of HeLa cells incubated with BHP (25  $\mu\text{M}$ ) (c) Fluorescence image of HeLa cells incubated with BHP (25  $\mu\text{M}$ ) alone (d) Fluorescence image of HeLa cells incubated with BHP (25  $\mu\text{M}$ ) and 25  $\mu\text{M}$  of  $\text{F}^-$  ions for 1 h

HeLa cells. Further, the HeLa cells were pre-treated with 25  $\mu\text{M}$  of **BHP** alone for 3 h. Then HeLa cells were seeded with 25  $\mu\text{M}$  of  $\text{F}^-$  ions for 1h. In the absence of  $\text{F}^-$  ions, the probe **BHP** exposed a weak yellow fluorescence. However, addition of  $\text{F}^-$  ions to the probe **BHP** induced a bright orange fluorescence (Figure 10). These results endorsed that the probe **BHP** can be successfully utilized for the intracellular fluorescence imaging analysis of  $\text{F}^-$  ions in HeLa cells.

Besides, the exceptional cell viability output of **BHP** has been further explored in four days Zebrafish embryos. Zebrafish has positioned as a well-known vertebrate model in numerous biological applications. From this perspective, we have utilized also zebrafish embryos as a living animal model to expose the excellent imaging potential of **BHP** for the detection of  $\text{F}^-$  ion in the biological environment (Figure 11).

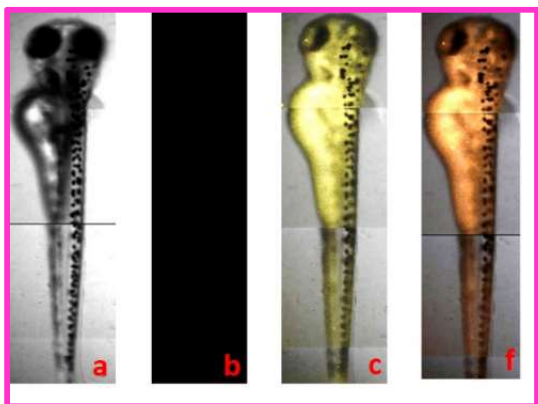


**Figure 11.** Fluorescence imaging analysis of  $\text{F}^-$  ion in 4 days old Zebrafish embryos developed with BHP and various concentrations of  $\text{F}^-$  ion (a) bright field images of BHP (25  $\mu\text{M}$ ) alone, (b) fluorescence merged images of BHP and  $\text{F}^-$  ion (25  $\mu\text{M}$ ) (c) fluorescence image of BHP (25  $\mu\text{M}$ ) alone (d) 25  $\mu\text{M}$  of  $\text{F}^-$  ion for 2 h continuously incubated with BHP (25  $\mu\text{M}$ ) for 3 h.

#### Evaluation of BHP with previous reports

The probe **BHP** has valid and multi features such as single step synthesis, dual-mode recognition, turn-on fluorescence response and colorimetric change. The probe **BHP** displayed unique sensing property among other dual sensors. Table S1 compares the sensing performance of **BHP** with recently reported  $\text{F}^-$  receptors. Amid, **BHP** exhibits too low limit of detection when compared with other previously reported chemoreceptors cited in table S1. Also, the limit of detection of **BHP** is within the range of recommended limits set by both EPA and WHO for  $\text{F}^-$  Ions. Moreover, the fluorescence imaging experiments inferred that the probe **BHP** can be utilized as potential tool for mapping  $\text{F}^-$  ion distribution in HeLa cells and Zebrafish embryos.

#### Conclusions

We have designed and synthesized a new chromogenic and fluorogenic probe based on salicylhydrazone derivative for the selective and sensitive detection of both  $\text{Cd}^{2+}/\text{F}^-$  ions by colorimetrically and fluorimetrically respectively. As per our knowledge, it is a novel simple hydrazone receptor for sensing carcinogenic heavy metal  $\text{Cd}^{2+}$  via colorimetric method and biologically significant  $\text{F}^-$  ion by both colorimetric and fluorimetric methods. The binding constant value of  $\text{Cd}^{2+}$  ion was found to be  $4.26 \times 10^{-4}$  M by UV-visible method where as  $6.03 \times 10^{-3}$  and  $3.01 \times 10^{-4}$  M for  $\text{F}^-$  ion by both UV-visible and fluorescence methods respectively. The limit of detection was found to be 0.05 nM for  $\text{F}^-$  ion. The excellent biological potential of **BHP** has been successfully utilized for the detection of  $\text{F}^-$  ions in Zebrafish embryos and human HeLa cells.

#### Acknowledgments

The authors acknowledge the financial support from the Council of Scientific and Industrial Research, Extramural Research, New Delhi, India (Grant No. 01(2901)17/EMR-II. The Department of Science and Technology, SERB, Extramural Major Research Project (Grant No. EMR/2015/000969), Department of Science and Technology, CERI, New Delhi, India (Grant No. DST/TM/CERI/C130(G) and we acknowledge the DST-FIST, DST-PURSE, DST-IRPHA, UPE programme and UGC-NRCBS, SBS, MKU for providing instrumentation facilities.

#### References

1. Jäkle, F. *Chem. Rev.* **2010**, 110, 3985.
2. Chen, X.; Zhou, Y.; Peng, X.; Yoon, J. *Chem. Soc. Rev.* **2010**, 39, 2120.
3. Kim, H.N.; Guo, Z.; Zhu, W.; Yoon J.; Tian, H. *Chem. Soc. Rev.* **2011**, 40, 79.
4. Zhang, J.F.; Zhou, Y.; Yoon, J.; Kim, J.S. *Chem. Soc. Rev.* **2011**, 40, 3416.
5. Zhou, Y.; Yoon, J. *Chem. Soc. Rev.* **2012**, 41, 52.
6. Chen, X.; Pradhan, T.; Wang, F.; Kim, J.S.; Yoon, J. *Chem. Rev.* **2012**, 112, 1910.
7. Wade, C.R.; Broomsgrove, A.E.J.; Aldridge, S.; Gabbaï, F.P. *Chem. Rev.* **2010**, 110, 3958.
8. Gale, P.A. *Chem. Soc. Rev.* **2010**, 39, 3746.
9. Wenzel, M.; Hiscock, J.R.; Gale P.A. *Chem. Soc. Rev.* **2012**, 41, 480.
10. Xu, Z.; Chen, X.; Kim, H.N.; Yoon, J. *Chem. Soc. Rev.* **2010**, 39, 127.
11. Galbraith, E.; James, T.D. *Chem. Soc. Rev.* **2010**, 39, 3831.
12. Xu, Z.; Kim, S.K.; Yoon, J. *Chem. Soc. Rev.* **2010**, 39, 1457.
13. Zhou, Y.; Xu, Z.; Yoon, J. *Chem. Soc. Rev.* **2011**, 40, 2222.
14. Quang, D.T.; Kim, J.S. *Chem. Rev.* **2010**, 110, 6280.

15. Zhou, Y.; Zhang, J.F.; Yoon, J. *Chem. Rev.* **2014**, 114, 5511.
16. Martínez-Mañez, R.; Sancenón, F. Fluorogenic and chromogenic chemosensors and reagents for anions, **2003**.
17. Waisberg, M.; Joseph, P.; Hale, B.; Beyersmann, D. *Toxicology.* **2003**, 192, 95.
18. McFarland, C.N.; Bendell-Young, L.I.; Guglielmo, C.; Williams, T.D. *J. Environ.Monit.* **2002**, 4, 791.
19. Nordberg, G. F.; Herber R. F. M.; Alessio, L. Cadmium in the Human Environment, Oxford University Press, Oxford, UK, **1992**.
20. Akula, M.; Thigulla, Y.; Nag, A.; Bhattacharya, A. *RSC Adv.* **2015**, 5, 57231.
21. Michael Kleerekoper. *Clin. North Am.* **2018**, 65, 441.
22. Erdal, S.; Buchanan, S.N.; *Environ. Health Perspect.* **2005**, 113, 111.
23. Michigami, Y.; Kuroda, Y.; Ueda, K.; Yamamoto, Y. *Anal. Chim. Acta.* **1993**, 274, 299.
24. Sivamani, J.; Siva, A. *Sens. Actuators, B*, **2017**, 242, 423.
25. Sarveswari, S.; JesinBeneto, A.; Siva, A. *Sens. Actuators, B*, **2017**, 245, 428.
26. Sivamani, J.; Sadhasivam, V.; Siva, A. *Sens. Actuators, B*. **2017**, 246, 108.
27. JesinBeneto, A.; Siva, A.; *Sens. Actuators, B.* **2017**, 247, 526.
28. Krishnaveni, K.; Iniya, M.; Jeyanthi, D.; Siva, A.; Chellappa, D. *Spectrochim. Acta A.* **2018**, 205, 557.
29. Krishnaveni, K.; Murugesan, S.; Siva, A. *New J. Chem.* **2019**, 4, 9021.
30. Krishnaveni, K.; Iniya, M.; Siva, A.; Vidhyalakshmi, N.; Ramesh, U.; Sasikumar, S.; Murugesan, S. *J. Mol. Struct.* **2020**, 1217, 128446.
31. Krishnaveni, K.; Harikrishnan, M.; Murugesan S.; Siva, A. *Microchem. J.* **2020**, 159, 105543.
32. Frisch, M. J.; Trucks, G. W.; Schlegel, H. B.; Scuseria, G. E.; Robb, M. A.; Cheeseman, J. R.; Scalmani, G.; Barone, B. Mennucci, G. A. Petersson, H. Nakatsuji, M. Caricato, V.; Li, X.; Hratchian, H. P.; Izmaylov, A. F.; Bloino, J.; Zheng, G.; Sonnenberg, J. L.; Hada, M.; Ehara, M.; Toyota, K.; Fukuda, R.; Hasegawa, J.; Ishida, M.; Nakajima, T.; Honda, Y.; Kitao, O.; Nakai, H.; Vreven, T.; Montgomery, J. A.; Peralta, J. E. Jr.; Ogliaro, F.; Bearpark, M.; Heyd, J. J.; Brothers, E.; Kudin, K. N.; Staroverov, V. N.; Kobayashi, R.; Normand, J.; Raghavachari, K.; Rendell, A.; Burant, J. C.; Iyengar, S. S.; Tomasi, J.; Cossi, M.; Rega, N.; Millam, J. M.; Klene, M.; Knox, J. E.; Cross, J. B.; Bakken, V.; Adamo, C.; Jaramillo, J.; Gomperts, R.; Stratmann, R. E.; Yazyev, O.; Austin, A. J.; Cammi, R.; Pomelli, C.; Ochterski, J. W.; Martin, R. L.; Morokuma, K.; Zakrzewski, V. G.; Voth, G. A.; Salvador, P.; Dannenberg, J. J.; Dapprich, S.; Daniels, A. D.; Farkas, O.; Foresman, J. B.; Ortiz, J. V.; Cioslowski, J.; Fox, D. J. Gaussian 09, Revision A.02, Gaussian, Inc., Wallingford CT, York, **1991**.